Monthly Notices
of the
ROYAL ASTRONOMICAL SOCIETY

Mon. Not. R. Astron. Soc. **418,** 2519–2526 (2011) doi:10.1111/j.1365-2966.2011.19642.x

Probing the internal rotation of pre-white dwarf stars with asteroseismology: the case of PG 0122+200

A. H. Córsico,[1,2]★ L. G. Althaus,[1,2] S. D. Kawaler,[3] M. M. Miller Bertolami,[1,2] E. García-Berro[4,5] and S. O. Kepler[6]

[1]*Facultad de Ciencias Astronómicas y Geofísicas, Universidad Nacional de La Plata, Paseo del Bosque s/n, (1900) La Plata, Argentina*
[2]*Instituto de Astrofísica La Plata (IALP-CONICET), Argentina*
[3]*Department of Physics and Astronomy, Iowa State University, 12 Physics Hall, Ames, IA 50011, USA*
[4]*Departament de Física Aplicada, Universitat Politècnica de Catalunya, c/Esteve Terrades 5, 08860 Castelldefels, Spain*
[5]*Institute for Space Studies of Catalonia, c/Gran Capità 2–4, Edif. Nexus 104, 08034 Barcelona, Spain*
[6]*Departamento de Astronomia, Universidade Federal do Rio Grande do Sul, Av. Bento Goncalves 9500 Porto Alegre 91501-970, RS, Brazil*

Accepted 2011 August 16. Received 2011 August 15; in original form 2011 July 13

ABSTRACT

We put asteroseismological constraints on the internal rotation profile of the GW Vir (PG1159-type) star PG 0122+200. To this end we employ a state-of-the-art asteroseismological model for this star and assess the expected frequency splittings induced by rotation adopting a forward approach in which we compare the theoretical frequency separations with the observed ones assuming different types of plausible internal rotation profiles. We also employ two asteroseismological inversion methods for the inversion of the rotation profile of PG 0122+200. We find evidence for differential rotation in this star. We demonstrate that the frequency splittings of the rotational multiplets exhibited by PG 0122+200 are compatible with a rotation profile in which the central regions are spinning about 2.4 times faster than the stellar surface.

Key words: stars: evolution – stars: individual: PG 0122+200 – stars: oscillations – stars: interiors – stars: rotation – white dwarfs.

1 INTRODUCTION

The upper-left corner of the Hertzsprung–Russell diagram is populated by a handful of rapidly variable stars, the so-called GW Vir stars. They are very hot and luminous, hydrogen-deficient pre-white dwarf stars characterized by surface layers rich in helium, carbon and oxygen (Werner & Herwig 2006) that exhibit non-radial g(gravity) modes with periods between 5 and 50 min – see e.g. Winget & Kepler (2008) and Althaus et al. (2010). In recent years, accurate asteroseismology of GW Vir stars has started to yield details of the internal structure and evolutionary status of these stars. On the observational side, the works of Vauclair et al. (2002) on RX J2117.1+3412, Fu et al. (2007) on PG 0122+200 and Costa et al. (2008) on PG 1159−035 are particularly noteworthy. On the theoretical front, important progress in the modelling of the internal structure of PG1159 stars (Althaus et al. 2005; Miller Bertolami & Althaus 2006) has made unprecedented asteroseismological inferences for GW Vir stars possible (Córsico et al. 2007a,b, 2008, 2009).

Asteroseismology of GW Vir stars provides information about the stellar mass, the chemical stratification, the luminosity and distance, and several other relevant properties such as stellar rotation rate and the presence and strength of magnetic fields. Of particular interest in the present investigation is the potential of asteroseismology to place constraints on stellar rotation, an important aspect that has been proved to be very difficult of assessing by means of traditional techniques – mostly spectroscopy. Specifically, rotation removes the intrinsic mode degeneracy of a non-radial g mode characterized by a harmonic degree ℓ and a radial order k. As a result, each pulsation frequency is split into multiplets of $2\ell + 1$ frequencies specified by different values of the azimuthal index m, with $m = 0, \pm 1, \ldots, \pm\ell$ (Unno et al. 1989). Rotational splittings in the power spectrum of a compact pulsator were first discovered in the white dwarf R 548 (Robinson, Nather & McGraw 1976). Since then, frequency splittings induced by rotation have been detected in a number of pulsating white dwarf and pre-white dwarf stars. If the rate of rotation is slow compared with the pulsation frequencies, the frequency separation between each component of the multiplet is proportional to the rotation velocity of the star. This has enabled us to derive the mean rotation period of a number of white dwarf and pre-white dwarf stars. Interestingly enough, this approach provides rotation velocities much more precise than those inferred from spectroscopy (Koester et al. 1998; Kawaler 2004).

Going one step forward the simple approach described above, Kawaler, Sekii & Gough (1999) were the first to explore the potential of the inversion methods employed in helioseismology to infer the internal rotation of PG 1159−035, the prototype of GW Vir stars. They found that PG 1159−035 could be rotating slightly faster at the centre than at the surface, but such a small contrast could

★E-mail: acorsico@fcaglp.unlp.edu.ar

also be compatible with rigid rotation within the uncertainties of the observed splittings. Kawaler et al. (1999) also compared the patterns of ($m = 0$) period spacings with the rotational splittings of PG 1159−035 and empirically found that the rotation rate of this star must increase with depth. Recently, Charpinet, Fontaine & Brassard (2009) have employed a forward approach aimed at determining the internal rotation profile of PG 1159−035. They fit the theoretical splittings corresponding to a model inspired in the asteroseismological (non-rotating) model of Córsico et al. (2008) to the observed frequency splittings of PG 1159−035. The forward approach of Charpinet et al. (2009) revealed that this star is rotating as a solid body with a rotation period of 33.61 ± 0.59 h.

In this paper, we perform a detailed asteroseismological study aimed at placing constraints on the internal rotation of PG 0122+200, the coolest known GW Vir star ($T_{\rm eff} = 80\,000 \pm 4000$ K and $\log g = 7.5 \pm 0.5$; Dreizler & Heber 1998), using the best existing evolutionary and seismic models. We present the observations and describe the seismological model of PG 0122+200 in Section 2. In Section 3 we explore the internal rotation of PG 0122+200 employing the forward approach. In Section 4 we perform rotation inversions for PG 0122+200 using the regularized least-squares (RLS) method (Section 4.1) and the function-fitting technique (Section 4.2). We conclude in Section 5 by summarizing our findings.

2 THE DATA AND THE MODEL

PG 0122+200 currently defines the locus of the low-luminosity red edge of the GW Vir instability strip. The photometric variations of this star were discovered by Bond & Grauer (1987). Some observational properties of PG 0122+200 are summarized in the second column of Table 1. We employ the high-quality observational data on PG 0122+200 gathered by Fu et al. (2007). They have presented multisite photometric observations of PG 0122+200 obtained with the Whole Earth Telescope (Nather et al. 1990) in 2001 and 2002. Using their data, together with those obtained in previous observational runs, they succeeded in detecting a total of 23 frequencies corresponding to modes with $\ell = 1$ and unambiguously derived a mean period spacing of 22.9 s. The 23 frequencies consist of seven rotational triplets ($m = -1$, 0, +1) and two isolated frequencies with (probably) $m = 0$. In Table 2, we show the seven triplets extracted from table 5 of Fu et al. (2007). The first three columns show the radial order, the harmonic degree and the azimuthal quantum number of the eigenmodes. The fourth and fifth columns give the pulsation periods and frequencies, respectively. The sixth column shows the uncertainty of the frequencies. Finally, in the seventh column the observed frequency splittings are listed, while the last column gives their uncertainties. The mean value (averaged on the seven triplets) of the frequency separations is 3.74 μHz. Adopting this value, Fu et al. (2007) derived a mean rotation period of 37.2 h.

Table 1. Properties of PG 0122+200.

Quantity	Spectroscopy	Asteroseismology
$T_{\rm eff}$ (kK)	80 ± 4^a	$81.54^{+0.8}_{-1.4}$
$M_\star$ ($M_\odot$)	0.53 ± 0.1^b	$0.556^{+0.009}_{-0.014}$
$\log g$ (cm s^{-2})	7.5 ± 0.5^a	$7.65^{+0.02}_{-0.07}$
$\log(L_\star/L_\odot)$	1.2 ± 0.5^c	$1.14^{+0.04}_{-0.02}$
$\log(R_\star/R_\odot)$	-1.67 ± 0.26^c	$-1.73^{+0.025}_{-0.01}$
$M_{\rm env}$ ($M_\odot$)	–	0.019 ± 0.006

[a]Dreizler & Heber (1998).
[b]Miller Bertolami & Althaus (2006).
[c]Estimated from $T_{\rm eff}$ and g, along with $M_\star$.

Table 2. The rotational triplets of PG 0122+200.

k	ℓ	m	$\Pi_{k\ell m}$ (s)	$\nu_{k\ell m}$ (μHz)	$\sigma[\nu_{k\ell m}]$ (μHz)	$\delta\nu^{\rm O}_{k\ell m}$ (μHz)	$\sigma[\delta\nu^{\rm O}_{k\ell m}]$ (μHz)
12	1	−1	336.28	2973.73	0.003		
						3.58	0.029
12	1	0	336.68	2970.15	0.029		
						3.60	0.030
12	1	+1	337.09	2966.55	0.007		
14	1	−1	379.55	2634.65	0.009		
						3.76	0.013
14	1	0	380.10	2630.89	0.009		
						3.87	0.015
14	1	+1	380.66	2627.02	0.012		
15	1	−1	400.41	2497.41	0.002		
						3.59	0.004
15	1	0	400.99	2493.82	0.003		
						3.58	0.004
15	1	+1	401.56	2490.24	0.003		
17	1	−1	448.79	2228.18	0.005		
						3.42	0.006
17	1	0	449.48	2224.76	0.004		
						3.36	0.004
17	1	+1	450.16	2221.40	0.002		
18	1	−1	467.87	2137.31	0.004		
						3.73	0.008
18	1	0	468.69	2133.58	0.007		
						3.49	0.009
18	1	+1	469.46	2130.09	0.005		
22	1	−1	562.70	1777.12	0.065		
						4.96	0.085
22	1	0	564.28	1772.16	0.056		
						4.10	0.074
22	1	+1	565.59	1768.06	0.049		
24	1	−1	609.64	1640.30	0.067		
						4.05	0.094
24	1	0	611.15	1636.25	0.067		
						3.28	0.078
24	1	+1	612.38	1632.97	0.040		

The theoretical rotational frequency splittings of PG 0122+200 were computed adopting the non-rotating asteroseismological model derived by Córsico et al. (2007b) on the basis of the modern set of PG 1159 fully evolutionary model sequences computed by Miller Bertolami & Althaus (2006). These models take into account the complete evolution of progenitor stars through the thermally pulsing asymptotic giant branch phase and born-again episode. Córsico et al. (2007b) constrain the stellar mass of PG 0122+200 by comparing the observed period spacing with the asymptotic period spacing and with the average of the computed period spacings. Finally, they employ the individual observed periods to find a representative seismological model for PG 0122+200. This asteroseismological model reproduces the $m = 0$ observed periods (see Table 2), with an average of the period differences (theoretical versus observed) of $\lesssim$0.9 s, and represents a substantial improvement over those models adopted in previous works. The characteristics of the asteroseismological model are compared with those obtained

spectroscopically in Table 1. As can be seen, the asteroseismological model accurately reproduces the observational data.

3 THE FORWARD APPROACH: ROTATIONAL SPLITTING FITS

Within this approach the theoretical frequency splittings obtained varying the assumed rotation profile are compared with the observational ones until a best global match is found (Charpinet et al. 2009). The goodness of the match between theoretical ($\delta\nu^{\rm T}_{k\ell m}$) and observed ($\delta\nu^{\rm O}_{k\ell m}$) rotational splittings is described using a quality function defined as

$$\chi^2 = \frac{1}{N_{\rm s}} \sum_{i=1}^{N_{\rm s}} \frac{1}{\sigma_i^2} \left(\delta\nu_i^{\rm T} - \delta\nu_i^{\rm O}\right)^2, \tag{1}$$

where we have replaced the subscripts (k, ℓ, m) with a single integer index i that labels the specific splitting ($i = 1, \ldots, N_{\rm s} \equiv 14$). Each term of the sum is weighted with the inverse square of the standard uncertainty (σ_i) of the observed splittings, which are derived from the uncertainties in the frequencies given in Fu et al. (2007) and are shown in the last column of Table 2. This is at variance with the preliminary study of Córsico & Althaus (2010), in which the fits of the rotational splitting were made without weighting the terms of the sum, and so the impact of the different uncertainties of the observational data on the final result was neglected. The lower the value of χ^2, the better the match between the theoretical and the observed frequency splittings.

The theoretical rotational splittings are computed using the expressions resulting from the perturbative theory to the first order in Ω (the rotation rate) that assumes that the pulsating star rotates with a period ($P \equiv 1/\Omega$) much longer than any of its pulsation periods (Unno et al. 1989). Under the assumption of rigid rotation (Ω constant), the theoretical frequency splittings are given by

$$\delta\nu^{\rm T}_{k\ell m} = -m\Omega\,(1 - C_{k\ell}), \tag{2}$$

with $m = 0, \pm1, \ldots, \pm\ell$, and $C_{k\ell}$ being the coefficients that depend on the eigenfunctions of the pulsation mode obtained in the non-rotating case. Such coefficients are computed as (Unno et al. 1989)

$$C_{k\ell} = \frac{\int_0^{\rm R_\star} \rho r^2 \left[2\xi_{\rm r}\xi_{\rm t} + \xi_{\rm t}^2\right] {\rm d}r}{\int_0^{\rm R_\star} \rho r^2 \left[\xi_{\rm r}^2 + \ell(\ell+1)\xi_{\rm t}^2\right] {\rm d}r}, \tag{3}$$

where $\xi_{\rm r}$ and $\xi_{\rm t}$ are the unperturbed radial and tangential eigenfunctions, respectively. In the case of g modes, when k is larger, then $\xi_{\rm r} \ll \xi_{\rm t}$, in such a way that $C_{k\ell} \to 1/\ell(\ell+1)$ (Brickhill 1975).

If the condition of rigid-body rotation is relaxed and (spherically symmetric) differential rotation is assumed, $\Omega = \Omega(r)$, the frequency splittings are given by (Unno et al. 1989)

$$\delta\nu^{\rm T}_{k\ell m} = -m \int_0^{\rm R_\star} \Omega(r) K_{k\ell}(r)\, {\rm d}r, \tag{4}$$

with $K_{k\ell}(r)$ being the first-order rotation kernels computed from the rotationally unperturbed eigenfunctions as (Unno et al. 1989)

$$K_{k\ell}(r) = \frac{\rho r^2 \left\{\xi_{\rm r}^2 - 2\xi_{\rm r}\xi_{\rm t} - \xi_{\rm t}^2\left[\ell(\ell+1) - 1\right]\right\}}{\int_0^{\rm R_\star} \rho r^2 \left[\xi_{\rm r}^2 + \ell(\ell+1)\xi_{\rm t}^2\right] {\rm d}r}. \tag{5}$$

From equation (4), it is clear that the frequency splitting for a given mode is just a weighted average of the rotation rate $\Omega(r)$ throughout the star, being the rotation kernel $K_{k\ell}(r)$ precisely the weighting function.

Note that the perturbative theory to the first order in Ω predicts symmetric separations of the $m \neq 0$ components within each multiplet with respect to the central one ($m = 0$) (see equations 2 and 4). Therefore, in this work we are neglecting the departures from symmetric frequency splitting within the triplets centred at $\Pi \sim 560$ s and $\Pi \sim 610$ s exhibited by PG 0122+200.[1]

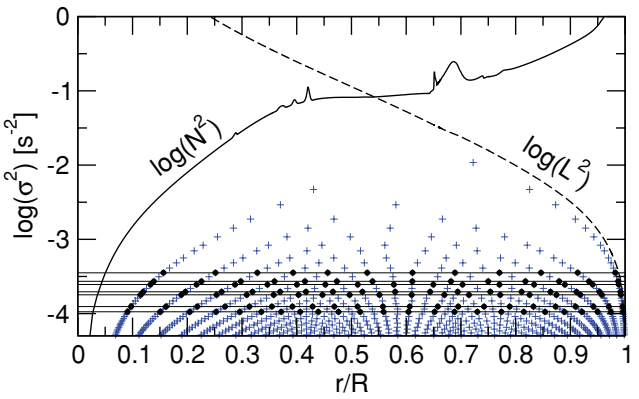

Figure 1. A propagation diagram of PG 0122+200 showing the logarithm of the squared Brunt–Väisälä (solid line) and Lamb (dashed line) frequencies. Also depicted is the location of the radial nodes of g modes (blue plus). The loci of the nodes corresponding to the modes exhibited by PG 0122+200 are emphasized with black dots and connected with horizontal lines.

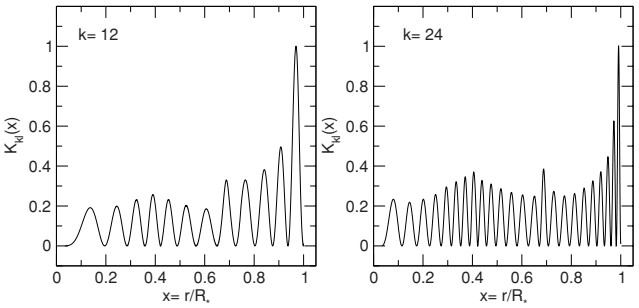

Figure 2. The normalized rotation kernel $K_{k\ell}(r)$ for the case of $k = 12$ (left) and $k = 24$ (right).

To estimate the region of the star probed by the observed g modes, we first examined a propagation diagram of the asteroseismological model of PG 0122+200. In Fig. 1, we plot the logarithm of the squared Brunt–Väisälä and the Lamb frequencies, along with the location of the nodes corresponding to g modes (the zeros of the radial eigenfunctions) marked with (blue) plus symbols. The nodes associated with the eigenmodes exhibited by PG 0122+200 are emphasized with black dots. Note that these modes have nodes in the region $0.1 \lesssim r/R_\star \lesssim 1$, implying that they have an oscillatory character in almost the whole star. We also examined the rotational kernels computed from our asteroseismological model for PG 0122+200. In Fig. 2, we show the normalized $K_{k\ell}(r)$ for $k =$ 12 and 24, corresponding to the shortest and the longest pulsation periods observed in PG 0122+200. As can be seen, the rotation kernels have the largest amplitudes at the outer regions of the model, but also have appreciable amplitudes (up to $\approx$0.3) throughout the *full* model of PG 0122+200, implying that the observed g modes

[1] There exists a number of reasons for these departures (see Vauclair et al. 2002), for instance, the presence of a magnetic field. The additional frequency shift due to a magnetic field is dependent on m^2, and thus, it could produce an asymmetry in the frequency shifts of the $m = +1$ and -1 components relative to the $m = 0$ component.

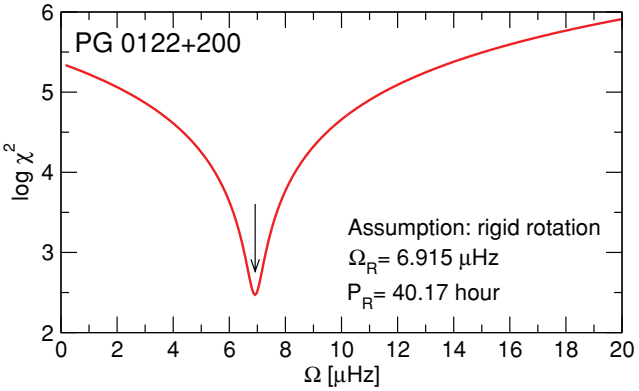

Figure 3. The quality function χ^2 in terms of the rotation rate Ω for the case in which we assume that PG 0122+200 rotates as a rigid body. Note the presence of a well-defined solution corresponding to $\Omega = 6.915$ μHz (arrow).

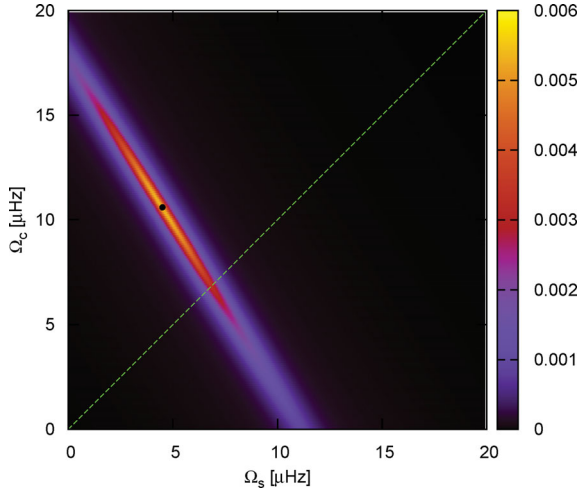

Figure 4. Contour map of the inverse of the quality function χ^2 showing the goodness of the fits in the Ω_s–Ω_c plane. We assume that PG 0122+200 rotates according to a linear profile. The colour scale is related to the value of $1/\chi^2$. Light regions are associated with the highest values of $1/\chi^2$, i.e. the best matches between observed and theoretical frequency splittings. The location of the best-fitting solution is shown with a black dot. The green dashed line indicates the loci of solutions corresponding to rigid rotation.

are sensitive to the entire rotation profile. This is in contrast to the case of DBV or DAV stars, in which rotational kernels sample only the outer regions of the star – see Kawaler et al. (1999) – because of the larger degeneracy of the core.

3.1 Rigid rotation

First, we assumed that PG 0122+200 rotates as a rigid body, that is, the rotation rate Ω is constant throughout the star. We have variated the value of Ω from 1.15×10^{-7} Hz ($P \sim 100$ d) to 2.77×10^{-4} Hz ($P \sim 1$ min), and for each value of Ω we computed the theoretical frequency splittings ($\delta\nu^{\rm T}_{k\ell m}$) by means of equation (2), where the coefficients $C_{k\ell}$ were assessed for each mode through equation (3) and not by means of the asymptotic relation, $C_{k\ell} \approx 1/\ell(\ell+1)$. The results of this optimization procedure are shown in Fig. 3 that shows the χ^2 function versus the rotation rate. The best-fitting solution corresponds to a rotation rate of $\Omega = 6.915$ μHz. It corresponds to a rotation period of $P = 40.17$ h, which is in good agreement with the approximate value of $P = 37.2$ h quoted by Fu et al. (2007). Note that the rotation period (of the order of 10^5 s) is much longer than the longest pulsation period exhibited by PG 0122+200 (∼600 s), thus justifying the use of the perturbative theory to a first order in the calculation of $\delta\nu^{\rm T}_{k\ell m}$.

3.2 Differential rotation

Here, we lift the assumption of solid-body rotation. Because of the exploratory nature of this study, we try very simplified functional forms for $\Omega(r)$. Specifically, we adopt a family of *linear* differential rotation profiles defined

$$\Omega(r) = (\Omega_{\rm s} - \Omega_{\rm c})r + \Omega_{\rm c}, \qquad (6)$$

where $\Omega_{\rm s}$ and $\Omega_{\rm c}$ are the rotation rates at the stellar surface and centre, respectively.[2] This family of linear profiles includes rotation rates that decrease and increase linearly with r and also 'flat' rotation profiles (when $\Omega_{\rm s} = \Omega_{\rm c}$) that represent the case of rigid rotation already examined in Section 3.1. We performed our optimization procedures varying the parameters $\Omega_{\rm s}$ and $\Omega_{\rm c}$ in the range 0–20 μHz. We computed the theoretical frequency splittings by means of equation (4), where the rotation kernels are computed by using equation (5). The results are shown in Fig. 4, where we prefer to plot $1/\chi^2$ instead of χ^2 to emphasize the location of the values ($\Omega_{\rm c}$, $\Omega_{\rm s}$), providing good agreement between observed and theoretical frequency splittings. The region of good solutions (that is, the smallest values of χ^2) has an elongated shape. As can be seen, there exists a unique, well-localized best-fitting solution at ($\Omega_{\rm c}$, $\Omega_{\rm s}$) = (10.62, 4.41) μHz, marked with a black dot in the plot. This solution is substantially different from rigid rotation, which should fall at some point along the green dashed line. The existence of the best-fitting solution suggests that the central regions of PG 0122+200 could be rotating more than twice faster than the surface.

We studied the sensitivity of our result to each of the observed rotational triplets. To this end, we have performed a simple experiment: we removed one of the observed triplets from our computations, keeping the six remainder, and searched for a solution. We started with the $k = 22$ complex that naively could be thought to have the strongest influence on our results due to its large frequency separations. Indeed, with an average frequency spacing of 4.53 μHz, it is significantly larger than the other spacings (see Table 2). We again find differential rotation with the core spinning more than twice faster than the surface, with the variations in the values of $\Omega_{\rm s}$ and $\Omega_{\rm c}$ being negligible when compared with the case in which all the seven splittings are taken into account. In fact, in this case, we have $\Omega_{\rm c} = 10.75$ μHz and $\Omega_{\rm s} = 4.40$ μHz. The similarity of the solutions is due to its large observational uncertainty, which, according to equation (1), strongly attenuates its impact. A similar experiment in which we remove the $k = 24$ triplet leads to very similar results. Clearly, these two triplets, which suffer from the largest uncertainties in the list, have no appreciable influence on our results. We repeated this experiment with the rest of the splittings. We found that the most critical triplets are, in the order of decreasing importance, $k = 18$, 17, 14 and 15. The frequency

[2] We have also tried two-zone rotation profiles like those used by Charpinet et al. (2009) for PG 1159−035, but we were unable to derive meaningful properties of the rotation of PG 0122+200, which is symptomatic of the inadequacy of the two-zone rotation profiles to represent the internal rotation of PG 0122+200.

separations for these triplets are accurately known. In particular, if we discard the $k = 18$ triplet, the solution becomes $\Omega_c = 16.45$ μHz and $\Omega_s = 0.95$ μHz, that is, strong differential rotation. On the other hand, if the $k = 17$ triplet is not considered, the solution turns out to be compatible with rigid rotation, with $\Omega_c = 7.70$ μHz and $\Omega_s = 6.55$ μHz. Hence, our results rely mostly on these two triplets, for which the frequency spacings are well determined (although see Section 3.4).

Finally, we examined the quality of the match between the observed and theoretical frequency splittings. We find that the best-fitting solution reproduces the observed frequency splittings with a mean difference of ≈0.25μHz, which is reduced to ≈0.1μHz when we do not consider the difference corresponding to the $k = 22$ triplet.

3.3 Uncertainties

In order to assess the uncertainties in the derived parameters, we repeated our optimization procedure adding artificial, normally (Gaussian) distributed uncertainties to the set of 14 observed splittings, with a standard deviation of $\sigma_{\rm noise} = 0.08$ μHz, which is comparable with the best data available for pulsating white dwarf and pre-white dwarf stars observed with the Whole Earth Telescope (Kawaler et al. 1999). We performed about 400 realizations of this type. The resulting solutions are shown in the left-hand panel of Fig. 5 with blue dots. Assuming that the distribution of solutions (Ω_c, Ω_s) is also Gaussian, we can estimate its dispersion, σ. We find that the solutions that deviate more from the best-fitting solution (free of uncertainties, black circle) are located at more than 2σ from the line that defines the solutions of rigid-body rotation (green line). In other words, rigid rotation can be discarded at a level of confidence of more than 2σ. We find $\Omega_c = 10.62 \pm 1.8$ μHz and $\Omega_s = 4.41 \pm 1.1$ μHz. We have repeated the above analysis adopting a deviation of $\sigma_{\rm noise} = 0.12$ μHz for the distribution of uncertainties in the frequency splittings (right-hand panel in Fig. 5). These artificial uncertainties are by far larger than the average of the uncertainties in frequencies quoted by Fu et al. (2007) in their table 4. Even in this extreme case, we can discard uniform rotation at a level of confidence of more than 1.5σ. Thus, the conclusion of differential rotation for PG 0122+200 remains unchanged even when we consider exaggerated uncertainties in the measured frequency splittings. Finally, we investigated the effects of uncertainties in the asteroseismological model on our results, and we found that they are not relevant.

3.4 The drift of the oscillation frequencies

Vauclair et al. (2011) have published the results of a comprehensive monitoring of seven oscillation frequencies of this star. They have reported changes of these oscillation frequencies over time, with much larger amplitudes and shorter time-scales than those expected by cooling, although the data resolution is rather low, of the order of 1 μHz. We focus on table 4 of Vauclair et al. (2011), which shows the frequency and amplitude variations of the seven largest amplitude modes of PG 0122+200 corresponding to the triplets centred at 2224 μHz ($k = 17$) and 2493 μHz ($k = 15$). These two triplets are the only ones (out of seven triplets present in the star) which have been well documented to exhibit changes over time.

From table 4 of Vauclair et al. (2011), we have computed the average value of the rotational shifts for each triplet as

$$\overline{\delta\nu}(t_n) = \overline{\delta\nu}_n = \frac{\delta\nu_{(+)} + \delta\nu_{(-)}}{2},$$

where $\delta\nu_{(+)} = \nu_{(m=+1)} - \nu_{(m=0)}$ and $\delta\nu_{(-)} = \nu_{(m=0)} - \nu_{(m=-1)}$ at a given epoch t_n of the observation, where $n = 1, \ldots, N_{\rm obs}$, being $N_{\rm obs} = 6$ for the triplet centred at 2224 μHz and $N_{\rm obs} = 8$ for the triplet centred at 2493 μHz. In this way, we discard the effects of the observed asymmetries in the frequency splittings within both triplets of PG 0122+200. This is consistent with the fact that, in this work, we are using the perturbative theory to the first order in Ω to estimate the frequency splittings that indeed does not account for possible departures of the uniformity of the splittings within a given multiplet (see Section 3). Next, we estimated an average value of

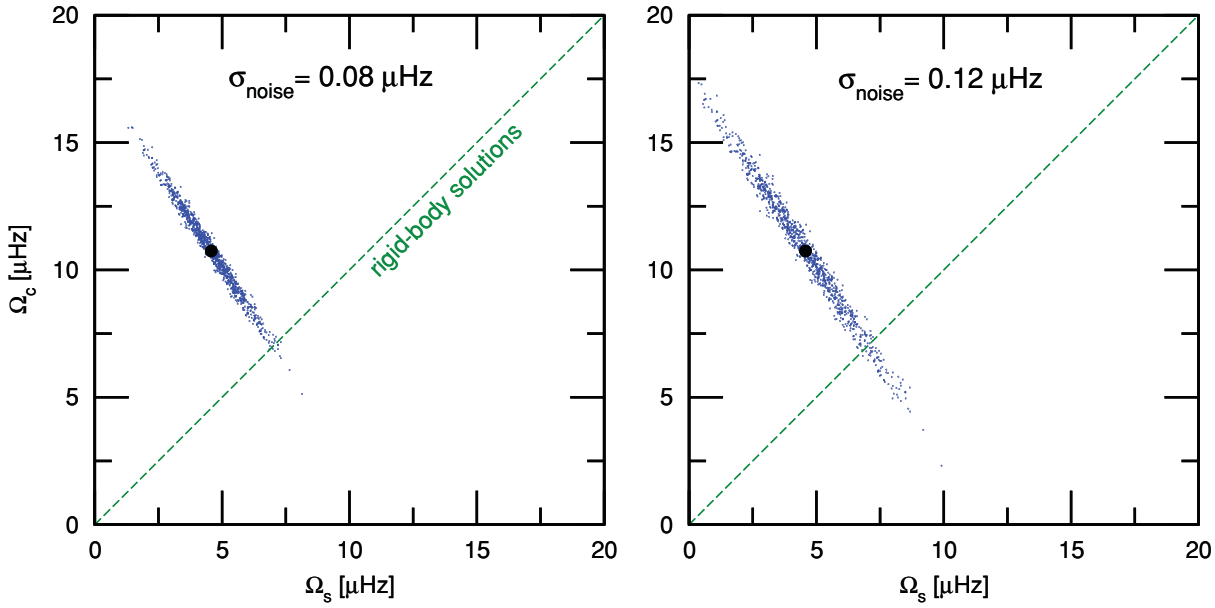

Figure 5. The best-fitting solution without uncertainties (black small circle) and the best-fitting solution corresponding to 400 realizations of the optimization procedure that include artificial noise (blue dots) with different standard deviations ($\sigma_{\rm noise}$). The green line indicates the loci of solutions of rigid rotation, where ($\Omega_c = \Omega_s$).

the splittings over the complete set of observations, namely

$$\langle\overline{\delta\nu}\rangle = \frac{1}{N_{\rm obs}}\sum_{n=1}^{N_{\rm obs}}\overline{\delta\nu}_n,$$

and the fluctuations around this value $\Delta_n = \overline{\delta\nu}_n - \langle\overline{\delta\nu}\rangle$ ($n = 1, \ldots, N_{\rm obs}$). Finally, we computed the mean value of these fluctuations around the average value

$$\langle\Delta_n\rangle = \frac{1}{N_{\rm obs}}\sum_{n=1}^{N_{\rm obs}}|\Delta_n|$$

and the variance of the fluctuations

$$\sigma_{\Delta_n} = \sqrt{\frac{1}{N_{\rm obs}}\sum_{n=1}^{N_{\rm obs}}(\Delta_n)^2}.$$

We find for the two triplets $\langle\Delta_n\rangle = 0.106$–$0.113$ μHz and $\sigma_{\Delta_n} = 0.05$–0.06 μHz.

We check our results of non-rigid rotation by considering these possible variations of the rotational splittings. We have performed new simulations of our optimization procedure, in each of them adding Gaussian noise to the splittings of the seven triplets exhibited by the star, with a standard deviation $\sigma_{\rm noise}$. To be consistent, we should adopt $\sigma_{\rm noise} \approx \sigma_{\Delta_n} \sim 0.055$ μHz in order to estimate the uncertainties of the frequency splittings due to the observed time variations, but we prefer to be somewhat conservative and adopt $\sigma_{\rm noise} \approx \langle\Delta_n\rangle \sim 0.11$ μHz, thus overestimating to some extent the impact of the frequency drifts on our results.[3] As expected, the results of our simulations are very similar to those shown in the right-hand panel of Fig. 5, indicating that rigid-body rotation can be discarded at a level of confidence of more than $\sim 1.5\sigma$.

4 THE INVERSE PROBLEM

4.1 The RLS inversion fits

We also investigated the internal rotation rate of PG 0122+200 using the RLS-fitting technique (Kawaler et al. 1999) that has been extensively applied to the case of the Sun – see Christensen-Dalsgaard, Schou & Thompson (1990) and references therein. In this method, the internal rotation profile $\Omega(r)$ is obtained by inverting the equation (Jeffrey 1988):

$$\delta\nu_i^{\rm O} = \int_0^{R_\star}\Omega(r)K_i(r)\,{\rm d}r, \qquad (7)$$

where $\delta\nu_i^{\rm O}$ is the ith observed frequency separation ($i = 1, \ldots, M$, where M is the number of observed multiplets). Here, $\delta\nu_i^{\rm O}$ corresponds to the average separation within a given multiplet. Because the problem is intrinsically ill posed, the inversion of the above equation necessarily must be regularized (Jeffrey 1988; Kawaler et al. 1999). To do so, we minimize

$$S = \sum_{i=1}^{M}\frac{1}{\sigma_i^2}\left[\delta\nu_i^{\rm O} - \delta\nu_i^{\rm T}\right]^2 + \lambda\int_0^R[\mathcal{L}\Omega(r)]^2\,{\rm d}r, \qquad (8)$$

where the second term of the right-hand side is, precisely, the regularization term. The form of the regularization term determines some additional constraints to the solution. For instance, if $\Omega(r)$ cannot have a steep spatial gradient, then $\mathcal{L} \equiv {\rm d}/{\rm d}r$. On the other hand, if $\Omega(r)$ must be smooth, then $\mathcal{L} \equiv {\rm d}^2/{\rm d}r^2$. The theoretical splittings $\delta\nu_i^{\rm T}$ are computed numerically:

$$\delta\nu_i^{\rm T} = \int_0^{R_\star}\Omega(r)K_i(r)\,{\rm d}r \approx \sum_{j=1}^{N}w_jK_{ij}\Omega_j, \qquad (9)$$

where $\Omega_j = \Omega(r_j)$ and $K_{ij} = K_i(r_j)$, with the index j ($j = 1, \ldots, N$) being associated with the radial mesh point in the stellar model on which the kernel $K_i(r)$ and the rotation rate $\Omega(r)$ are evaluated, and $w_j = r_{j+1} - r_j$.

In the least-squares method, the derivative of the sum of the squared residuals (the function S) with respect to Ω_j is taken and equated to zero. After some algebra, the following matrix equation is derived:

$$(\mathbf{K}^{\rm T}\mathbf{K} + \lambda\mathbf{H})\boldsymbol{\Omega} = \mathbf{K}^{\rm T}\boldsymbol{\Upsilon}, \qquad (10)$$

where $\mathbf{K}$ is an $(N \times M)$ matrix with elements $(\mathbf{K})_{ij} = w_jK_{ij}/\sigma_i$, $\boldsymbol{\Omega}$ is an $(N \times 1)$ vector with components $(\boldsymbol{\Omega})_j = \Omega_j$, and $\boldsymbol{\Upsilon}$ is an $(M \times 1)$ vector with components $(\boldsymbol{\Upsilon})_i = \delta\nu_i^{\rm O}/\sigma_i$. Finally, $\mathbf{H}$ is the $(N \times N)$ regularization matrix, which adopts a tridiagonal form (that is, $(\mathbf{H})_{ij} = 0$ for $|i-j| > 1$) or a pentadiagonal structure (that is, $(\mathbf{H})_{ij} = 0$ for $|i-j| > 2$) depending on whether $\mathcal{L} \equiv {\rm d}/{\rm d}r$ or $\mathcal{L} \equiv {\rm d}^2/{\rm d}r^2$. Equation (10) constitutes an $(N \times N)$ system of linear equations that must be solved for the unknown rotation velocities Ω_j that minimize S.

We have tested the reliability of our RLS scheme by employing this technique on 'synthetic' (free of uncertainties) frequency splittings generated with the asteroseismological model of PG 0122+200 through the forward approach. Specifically, we considered rotational splittings corresponding to consecutive $\ell = 1$ g modes with $k = 1, \ldots, 40$. We employed the LU decomposition and also the Gauss–Jordan methods (Press et al. 1992) for solving the system. Both methods give almost identical results. In all of the cases we have examined, the inversions are able to recover the input rotation profile that we used to compute the synthetic splittings, provided that an adequate range of values of the parameter λ is adopted.

We have applied the RLS method to infer the internal rotation profile of PG 0122+200. We have employed the $M = 7$ averaged $\ell = 1$ splittings. The regularization matrix corresponds to the smoothing of the second derivative of $\Omega(r)$. In Fig. 6, we show the inverted rotation profiles for PG 0122+200 for several values of λ. For very small values of λ, the inverted profiles exhibit strong variations that

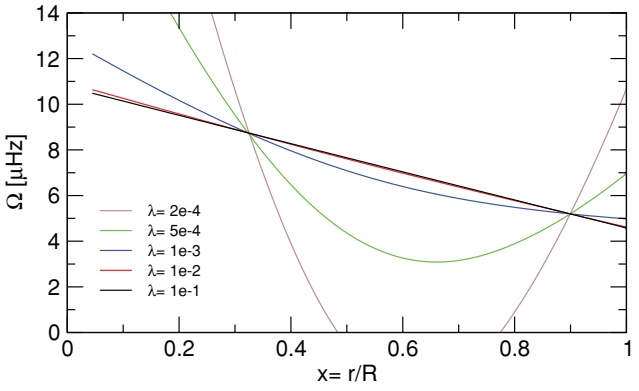

Figure 6. Inverted rotation profiles for PG 0122+200 corresponding to different values of the regularization parameter λ.

[3] Note that this is actually an estimation of the magnitude of time variations of the frequency separations of PG 0122+200 because we do not know the changes that could be experiencing the frequencies and frequency separations that have not been monitored by Vauclair et al. (2011).

lack physical meaning. However, as the value of λ is increased, the inverted solution gradually stabilizes. The resulting rotation profile (corresponding to $\lambda \gtrsim 10^{-2}$) consists of an almost linearly decreasing rotation rate with $\Omega_c \sim 10.75$ μHz and $\Omega_s \sim 4.58$ μHz, in excellent agreement with the results of the forward approach. The monotonic linear functional form characterizing the inverted rotation profiles should not be surprising, since we are forcing $\Omega(r)$ to have a small value of its second derivative at the outset. An analysis of the uncertainties similar to that performed for the forward approach leads to the conclusion that even with the inclusion of uncertainties in the observed splittings, the rotation of PG 0122+200 is faster at the central regions than at the surface. Specifically, we found $\Omega_c = 10.75 \pm 2.4$ μHz and $\Omega_s = 4.58 \pm 1.7$ μHz.

4.2 The function-fitting method

We have also made rotational inversions on to a fixed functional basis – a method called 'function fitting', see Kawaler et al. (1999) for details. In this inversion technique, an explicit assumption about the functional form of $\Omega(r)$ is made. For instance, if $\Omega(r)$ is assumed to be a polynomial in r of degree $K-1$, then $\Omega(r) = \sum_{k=1}^{K} a_k r^{k-1}$. Following the least-squares method, in which we minimize the sum of the squared residuals, we obtain the matrix equation

$$(\mathbf{A}^{\mathrm{T}}\mathbf{A})\boldsymbol{a} = \mathbf{A}^{\mathrm{T}}\boldsymbol{\Upsilon}, \tag{11}$$

where $\mathbf{A}$ is an $(M \times K)$ matrix with elements

$$(\mathbf{A})_{ik} = \sum_{j=1}^{N} \frac{1}{\sigma_i} w_j K_{ij} r_j^{k-1}, \tag{12}$$

$\boldsymbol{a}$ is a $(K \times 1)$ vector with components $(\boldsymbol{a})_k = a_k$ and $\boldsymbol{\Upsilon}$ is an $(M \times 1)$ vector with components $(\boldsymbol{\Upsilon})_i = \delta\nu_i^{\mathrm{O}}/\sigma_i$. Equation (11) is a $(K \times K)$ system of linear equations that must be solved for the unknown set of values of a_k that minimize S.

Specifically, we have explored linear ($K = 2$) functional forms for $\Omega(r)$, defined by the two parameters $a_1 = \Omega_c$ and $a_2 = (\Omega_s - \Omega_c)$. The optimal values we found for these parameters are $\Omega_c = 10.74 \pm 2.9$ μHz and $\Omega_s = 4.57 \pm 1.8$ μHz, which is in excellent agreement with the RLS fits and also with the forward approach.

5 SUMMARY AND CONCLUSIONS

Reliable determinations of the rotation rate of white dwarf and pre-white dwarf stars are important because they can provide constraints on the theories of angular momentum transport from the core to the envelopes of their progenitors. These theories predict white dwarf rotation rates that are much larger than those spectroscopically found (Koester et al. 1998; Berger et al. 2005) and even larger than the rotation rates inferred from pulsating white dwarfs (Kawaler 2004), unless magnetic torques are taken into account (Suijs et al. 2008). These magnetic torques provide the necessary spin-down of the cores of the white dwarf progenitors, thus helping to understand the slow rotation of white dwarfs.

In this work, we have explored the internal rotation of the pulsating pre-white dwarf star PG 0122+200 on the basis of its observed frequency splittings employing a forward approach and also two rotation inversion techniques. The three methods employed in this work suggest that the internal rotation profile of PG 0122+200 is differential, with the central regions rotating more than twice faster than the stellar surface. Rigid-body rotation can be discarded for this star at a level of confidence of more than 1.5 and 2σ when we consider uncertainties in the observed frequency separations of 0.12 and 0.08 μHz, respectively. By averaging our results according to the three methods employed, we estimate that the core-to-surface rotation ratio is $\Omega_c/\Omega_s = 2.4 \pm 1.3$.

Up to now, only our Sun (Schou et al. 1998) and two pulsating β Cephei stars – HD 129929 (Dupret et al. 2004) and ν Eridani (Pamyatnykh, Handler & Dziembowski 2004) – are known to be rotating differentially with depth. Our results for PG 0122+200 can be considered as the first asteroseismic evidence of differential rotation with depth for an evolved star. Finally, the fact that the internal rotation profile of the prototypical star PG 1159−035, which is rotating as a rigid body, is apparently very different than that obtained here for PG 0122+200 could be indicative that PG1159 stars are the result of different evolutionary channels and different mass-loss histories, as suggested by recent theoretical evidence (Althaus et al. 2009). Our results call for the need of similar analysis for other well-studied GW Vir stars.

ACKNOWLEDGMENTS

Part of this work was supported by AGENCIA through the Programa de Modernización Tecnológica BID 1728/OC-AR, the PIP 112-200801-00940 grant from CONICET, MCINN grant AYA2008–04211–C02–01, the ESF EUROCORES Program EuroGENESIS (MICINN grant EUI2009-04170), the European Union FEDER funds and the AGAUR. This research has made use of NASA's Astrophysics Data System.

REFERENCES

Althaus L. G., Serenelli A. M., Panei J. A., Córsico A. H., Garcia-Berro E., Scoccola C., 2005, A&A, 435, 631
Althaus L. G., Panei J. A., Miller Bertolami M. M., García-Berro E., Córsico A. H., Romero A. D., Kepler S. O., Rohrmann R. D., 2009, ApJ, 704, 1605
Althaus L. G., Córsico A. H., García-Berro E., Isern J., 2010, A&AR, 18, 471
Berger L., Koester D., Napiwotzki R., Reid I. N., Zuckerman B., 2005, A&A, 444, 565
Bond H. E., Grauer A. D., 1987, ApJL, 321, L123
Brickhill A. J., 1975, MNRAS, 170, 405
Charpinet S., Fontaine G., Brassard P., 2009, Nat, 461, 501
Christensen-Dalsgaard J., Schou J., Thompson M. J., 1990, MNRAS, 242, 353
Córsico A. H., Althaus L. G., 2010, in Werner K., Rauch T., eds, AIP Conf. Proc. Vol. 1273, 17th European White Dwarf Workshop. Am. Inst. Phys, New York, p. 566
Córsico A. H., Althaus L. G., Miller Bertolami M. M., Werner K., 2007a, A&A, 461, 1095
Córsico A. H., Miller Bertolami M. M., Althaus L. G., Vauclair G., Werner K., 2007b, A&A, 475, 619
Córsico A. H., Althaus L. G., Kepler S. O., Costa J. E. S., Miller Bertolami M. M., 2008, A&A, 478, 869
Córsico A. H., Althaus L. G., Miller Bertolami M. M., García-Berro E., 2009, A&A, 499, 257
Costa J. E. S. et al., 2008, A&A, 477, 627
Dreizler S., Heber U., 1998, A&A, 334, 618
Dupret M.-A., Thoul A., Scuflaire R., Daszyńska-Daszkiewicz J., Aerts C., Bourge P.-O., Waelkens C., Noels A., 2004, A&A, 415, 251
Fu J.-N. et al., 2007, A&A, 467, 237
Jeffrey W., 1988, ApJ, 327, 987
Kawaler S. D., 2004, in Maeder A., Eenens P., eds Proc. IAU Symp. 215, Stellar Rotation. Astron. Soc. Pac., San Francisco, p. 561
Kawaler S. D., Sekii T., Gough D., 1999, ApJ, 516, 349
Koester D., Dreizler S., Weidemann V., Allard N. F., 1998, A&A, 338, 612

Miller Bertolami M. M., Althaus L. G., 2006, A&A, 454, 845
Nather R. E., Winget D. E., Clemens J. C., Hansen C. J., Hine B. P., 1990, ApJ, 361, 309
Pamyatnykh A. A., Handler G., Dziembowski W. A., 2004, MNRAS, 350, 1022
Press W. H., Teukolsky S. A., Vetterling W. T., Flannery B. P., 1992, Numerical Recipes in FORTRAN. The Art of Scientific Computing. 2nd edn. Cambridge Univ. Press, Cambridge
Robinson E. L., Nather R. E., McGraw J. T., 1976, ApJ, 210, 211
Schou J. et al., 1998, ApJ, 505, 390
Suijs M. P. L., Langer N., Poelarends A.-J., Yoon S.-C., Heger A., Herwig F., 2008, A&A, 481, L87
Unno W., Osaki Y., Ando H., Saio H., Shibahashi H., 1989, Nonradial Oscillations of Stars, 2nd edn. University of Tokyo Press, Tokyo
Vauclair G. et al., 2002, A&A, 381, 122
Vauclair G. et al., 2011, A&A, 528, A5
Werner K., Herwig F., 2006, PASP, 118, 183
Winget D. E., Kepler S. O., 2008, ARA&A, 46, 157

This paper has been typeset from a TEX/LATEX file prepared by the author.